

1 Link to publisher version: <https://doi.org/10.1016/j.ijhazmat.2020.123957>

2 **Chemical Recycling of Poly-(Bisphenol A Carbonate) by Diaminolysis:**
3 **a New Carbon-Saving Synthetic Entry into Non-Isocyanate Polyureas**
4 **(NIPUreas)**

5 Eugenio Quaranta^{a,b,*}, Angela Dibenedetto^{a,b}, Francesco Nocito^a, Paola Fini^c

6 ^a *Università degli Studi di Bari “Aldo Moro”, Dipartimento di Chimica, Campus Universitario, Via E. Orabona, 4,*
7 *70126, Bari, Italy*

8 ^b *Consorzio Interuniversitario “Reattività e Catalisi”, via Celso Ulpiani, 27, 70126, Bari, Italy*

9 ^c *Istituto per i Processi Chimico Fisici (IPCF-CNR) c/o Dipartimento di Chimica, Via Orabona, 4, 70126, Bari, Italy*

10

11

12

13

14

15

16

17

18

19

20 * Corresponding author. *Phone:* (+39) 080 5442093.

21 *E-mail address:* eugenio.quaranta@uniba.it (E. Quaranta).

22

23 ABSTRACT

24 The present study describes an unprecedented approach to valorize potentially hazardous poly-
25 (bisphenol A carbonate) (PC) wastes. In THF, under non-severe conditions (120 °C), the reaction of
26 PC with long-chain diamines H₂NRNH₂ (2 equivalents) provided a tool to regenerate the monomer
27 bisphenol A (BPA; 83-95%, isolated) and repurpose waste PC into [-NHRNHCO-]_n polyureas
28 (PUs; 78-99%, isolated) through a non-isocyanate route. Basic diamines (1,6-diaminohexane,
29 4,7,10-trioxa-1,13-tridecanediamine, *meta*-xylylenediamine, *para*-xylylenediamine) reacted with
30 PC without any auxiliary catalyst; less reactive aromatic diamines (4,4'-diaminodiphenylmethane,
31 2,4-diaminotoluene) required the assistance of a base catalyst (1,8-diazabicyclo[5.4.0]undec-7-ene,
32 NaOH). The formation of [-NHRNHCO-]_n goes through a carbamation step affording BPA and
33 carbamate intermediates H[-OArOC(O)NHRNHC(O)-]_nOArOH (Ar = 4,4'-C₆H₄C(Me)₂C₆H₄-)
34 that, in a subsequent step, convert into [-NHRNHCO-]_n and more BPA. All the PUs were
35 characterized in the solid state by CP/MAS ¹³C-NMR (δ(C=O) = 152-161 ppm) and IR
36 spectroscopy. The positions of ν(N-H) and ν(C=O) absorptions are typical of "hydrogen-bonded
37 ordered" bands supporting the presence of H-bonded groups in network structures characterized by
38 some degree of order or regularity. DSC and TGA analyses showed that the PUs are thermally
39 stable (T_{d,5%}: 212-270 °C) and suitable for being processed since their degradation begins at
40 temperatures about 100 °C higher than their T_g or T_m.

41

42 *Keywords:* BPA; polycarbonate; polyureas; waste plastic valorization; circular economy

43

44

45 ABBREVIATIONS:

46 ATR: Attenuated Total Reflectance; BPA: 2,2-bis(4-hydroxyphenyl)propane, bisphenol A; CAGR:
47 Compound Annual Growth Rate; CP/MAS: Cross Polarization Magic-Angle Spinning; DBU: 1,8-
48 diazabicyclo[5.4.0]undec-7-ene; DSC: Differential Scanning Calorimetry; HMDA: 1,6-diaminohexane;
49 MDA: 4,4'-diaminodiphenylmethane; NIPUreas: Non-Isocyanate PolyUreas; PC: Poly-(bisphenol A
50 carbonate); PU: polyurea; TDA: 2,4-diaminotoluene; TGA: Thermogravimetric Analysis; TMS:
51 tetramethylsilane; TOSS: Total Sideband Suppression; TOTDA: 4,7,10-trioxa-1,13-tridecanediamine;
52 UR(PC): repeating unit of PC; *m*-XYLDA: *meta*-xylylenediamine; *p*-XYLDA: *para*-xylylenediamine.

53 **1. Introduction**

54 Polymeric materials have experienced a widespread rapid diffusion in our daily life.
55 However, as a consequence of linear way of consuming plastics, these materials have been
56 accumulating in the environment and have generated health, environmental and social concerns that
57 make necessary a change of strategy, such as shifting to a circular and environmentally sustainable
58 plastic economy based on the recycling of these materials at the end of their life-cycle [La Mantia,
59 2002; Ragaert et al., 2017; Fortman et al., 2018]. In the last few years chemical recycling of plastics
60 has been gaining great attention as a methodological approach to reduce the environmental and
61 social impact of this type of wastes, providing thus a potential tool to generate a sustainable supply
62 chain for a variety of polymeric materials. This approach, that implies the chemical conversion of
63 the waste polymer into added-value chemicals, is not only a captivating alternative to landfill or
64 energy recovery, but also a smart response to the current worldwide need of saving carbon and
65 energy and protecting fossil resources from depletion [Datta and Kopczynska, 2016; Rahimi and
66 Garcia, 2017; Hong and Chen, 2017; Jehanno et al., 2019; Shao et al., 2020].

67 Poly-(bisphenol A carbonate) (PC), currently accessible through phosgeneless synthetic
68 routes [Kim, 2020], is one of the most widely used thermoplastics. PC global market is steeply
69 expanding and is projected to reach approximately 5.1 million tons by the end of 2023, increasing at
70 a CAGR of around 3% per year in the period 2017-2023 [Asscoated Press News, 2018]. The fast
71 increase of manufacture and utilization of PC raises the problem of the fate of the wastes of this
72 material. The polymer is a potential reservoir of 2,2-bis(4-hydroxyphenyl)propane (bisphenol A;
73 BPA), a known xenoestrogen and endocrine disruptor, that is potentially harmful to both wildlife,
74 including marine organisms, and humans [Tucker et al., 2018]. Prevention of BPA leaching into the
75 environment through uncontrolled hydrolysis or biodegradation of the waste polymer is matter that
76 deserves due attention as BPA release into the environment may have adverse repercussions on
77 many living organism and human health.

78 These concerns call for the development of environmentally friendly and cost-efficient post-
79 consumer PC treatments. Chemical recycling of waste PC can provide a convenient answer to this
80 issue, as it opens a way to the valorization of the waste polymer [Antonakou and Achilias, 2013;
81 Datta and Kopczynska 2016; Hong and Chen, 2017; Kim, 2020]. In this ambit different approaches
82 can be pursued, such as pyrolysis [Wang et al., 2020], reduction (hydrogenation, hydrosilylation)
83 [Monsigny et al., 2018; Westhues et al., 2018; Alberti et al., 2020a], or also other options based on
84 the chemical fission of carbonate bond by hydrolysis [Taguchi et al., 2016; Quaranta, 2017; Liu et
85 al., 2018], alcoholysis [Quaranta et al., 2017; Liu et al., 2019; Alberti et al., 2020b], phenolysis
86 [Alberti et al., 2019], glycolysis [Iannone et al., 2017; Quaranta et al., 2018; Do et al., 2018;
87 Jehanno et al., 2020], aminolysis [Hata et al., 2002; Singh et. al., 2015; Iannone et al., 2017; Wu et
88 al., 2018; Demarteaue et al., 2020]. The latter methods allow to regenerate the monomer, bisphenol
89 A, that can be reused to produce new virgin PC, or polymeric materials different from PC (for
90 instance, poly(aryl ether sulfone)s [Jones et al., 2016], or also converted into other products such
91 as, for example, jet fuel range high-density polycycloalkanes [Tang et al., 2019]. However, these
92 approaches can also cogenerate high added value chemicals besides BPA, such as carbonic acid
93 diesters or organic carbamates and ureas if the polymer is reacted respectively with alcohols or
94 amines. In the latter cases waste PC can be used as a carbonylating agent succedaneous of harmful
95 phosgene [Hata et al., 2003; Carafa and Quaranta, 2009].

96 Herein we have focused on the aminolysis reaction. Relative to other PC depolymerization
97 methods, the reaction of PC with amine substrates has received rather poor attention in the past and,
98 only occasionally, has been explored as a way to recycle the polymer (PC) chemically [Hata et al.,
99 2002; Singh et. al., 2015; Iannone et al., 2017; Wu et al., 2018; Demarteaue et al., 2020]. Depending
100 on the experimental conditions and the nature of amine (primary or secondary), the
101 depolymerization of PC with mono-amines can afford, besides BPA, carbamates or acyclic mono-
102 ureas $RR'NC(O)NRR'$ ($R = H$, $R' = \text{alkyl, aryl}$; $R = R' = \text{alkyl}$) in variable yields [Hata et al., 2002;
103 Singh et. al., 2015; Iannone et al., 2017; Demarteaue et al., 2020]. The reaction of the polycarbonate

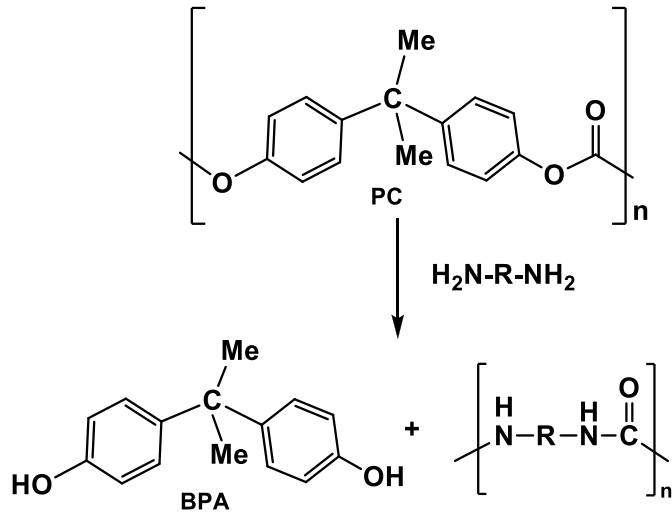
104 with short-chain diamines, such as *N,N'*-dimethyl-1,2-diaminoethane or *N,N'*-dimethyl-1,3-
105 diaminopropane, 1,2-diaminopropane, 1,3-diaminopropane, has been exploited for the synthesis of
106 the relevant cyclic ureas [Hata et al., 2002; Iannone et al., 2017]. Very recently, PC was reacted
107 with aliphatic primary diamines to give hydroxyl-*N,N'*-diphenylene-isopropylidene bis-carbamate
108 prepolymers that, in a subsequent Sn-catalyzed step, were chain-extended with commercially
109 available diisocyanates to produce a variety of polyurethanes [Wu et al., 2018].

110 Relative to the above studies [Hata et al., 2002; Singh et al., 2015; Iannone et al., 2017; Wu
111 et al., 2018; Demarteau et al., 2020], in this work we have followed an unprecedented approach to
112 valorize PC wastes as the reaction of PC with a few long-chain diamines has been explored as a
113 way to regenerate the monomer and, for the first time in the literature, repurpose waste PC into
114 virgin polyureas (PUs) straightforwardly, in a one-pot process (Fig. 1). In virtue of their special
115 properties (resistance to hydrolysis, oxidation and abrasion; excellent mechanical and anti-corrosion
116 properties; thermal stability at high temperatures; biocompatibility) polyureas have been finding
117 wide application in several fields (coatings, greases, membranes, microcapsules, biomedical
118 devices) [Pires et al., 2000]. Quite recently, these compounds have been successfully used as
119 starting materials for the phosgeneless synthesis of $R'O(O)CNHRNHC(O)OR'$ dicarbamates
120 [Shang et al., 2012], widely used in industry as precursors of polyurethanes.

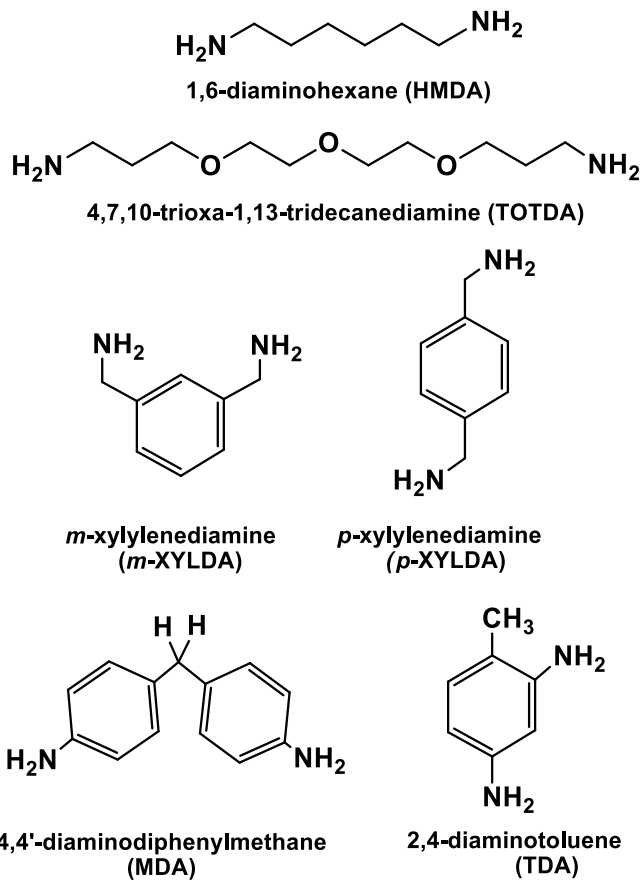
121 PUs are traditionally prepared by polyaddition of diamines and diisocyanates [Pires et al.,
122 2000]. The toxicity of isocyanates has urged both academia and industry to explore more
123 environmentally friendly isocyanate-free methods of synthesis of polyureas (Non-
124 IsocyanatePolyUreas (NIPUreas)): for instance, the reaction of diamines with carbonyl sources
125 such as carbon dioxide [Rockicki, 1988; Shang et al., 2012; Wu et al., 2012; Ying et al. 2015;
126 Wang et al., 2016], urea [Dennis et al., 2018], diphenyl carbonate [Pan et al., 2015], or also dialkyl
127 dicarbamates $R'O(O)CNHRNHC(O)OR'$ [Ma et al., 2018], that, recently, have been converted into
128 NIPUreas by metathesis polymerization in the presence of a base catalyst [Kébir et al., 2017].
129 Herein, we report on a new route to polyureas that, as an outstanding peculiarity, conjugates the

130 feature of avoiding any use of hazardous isocyanates with the advantages of recycling a potentially
 131 hazardous waste polymer (PC) and saving carbon (Fig. 1).

132



Diamines $\text{H}_2\text{N-R-NH}_2$ used



133

134

Fig. 1. Repurposing of waste PC into polyureas.

135 2. Experimental

136 2.1. General methods and materials

137 Vacuum line techniques were used for manipulations carried out under inert
138 atmosphere (N₂). THF and diethyl ether were dried according to standard procedures (P₂O₅;
139 Na/benzophenone) [Perrin et al., 1986]. 1,8-diazabicyclo[5.4.0]undec-7-ene (DBU) and the
140 diamines (Fig. 1) were from Aldrich and were used as received except HMDA that was
141 purified by sublimation before use. Both DBU and the basic diamines HMDA, TOTDA, *m*-
142 XYLDA, *p*-XYLDA were manipulated under N₂ to prevent any contamination from
143 atmospheric CO₂ or moisture. PC pellets (SABIC; 3 mm length × 2 mm diameter) were used
144 as a model of waste polycarbonate. The characterization of the polymer was reported
145 elsewhere [Quaranta et al., 2018]. The moles of BPA (n°_{BPA}) incorporated in w grams of
146 feed polycarbonate were assumed to be equal to the moles of repeating unit of PC (UR(PC)),
147 $n_{UR(PC)}$, and were calculated according to Eq. (1), where $MM_{UR(PC)}$ is the molar mass of the
148 UR(PC) (254.29 g/mol; Fig. 1).

$$149 \quad n^{\circ}_{BPA} = n_{UR(PC)} = w/MM_{UR(PC)} \quad (1)$$

150 GC analyses were performed with a THERMO Scientific TRACE 1310 gas-
151 chromatograph (GC column: Heliflex AT-5, 30 m × 0.25 mm, 0.25 μm film thickness). IR
152 spectra were taken on a Shimadzu FTIR Prestige 21 spectrophotometer or a Perkin Elmer
153 Frontier MIR/FIR spectrophotometer equipped with a Pike GladiATR (diamond crystal)
154 accessory. ¹³C NMR cross polarization magic angle scanning (CP/MAS) measurements
155 were performed at 151 MHz on a Bruker AVANCE 600 apparatus equipped with a MAS II
156 Pneumatic Unit, using TOSS technique. Solid sample was packed in a 4 mm zirconia rotor
157 with a Kel-F cap and spinning at 11 kHz during the analysis (delay time = 4 s). CP/MAS ¹³C
158 chemical shifts of solid samples are referenced to the resonance of adamantane at 29.5 ppm.
159 ¹H and ¹³C NMR chemical shifts of samples in solution are in δ (ppm) versus TMS. The

160 thermal properties of the polyureas were investigated by DSC (Q200 TA Instruments) and
 161 TGA (Pyris 1-Perkin Elmer) under a nitrogen flow of 50 mL/min at the heating rate of 10
 162 °C/min. The TGA experiments were performed from 40 °C to 800 °C. In the DSC
 163 experiments the samples were heated, cooled and heated again from 0 °C to a maximum
 164 temperature determined by the thermal stability of each sample, as evaluated by TGA
 165 measurements. The first DSC heating run was used to remove any thermal effect that may
 166 hide transitions such as, for instance, glass transitions or melting. Glass temperature was
 167 determined at the inflection of the step in the baseline, whereas the melting temperature at
 168 the maximum of the endothermic peak. Both DSC and TGA measurements were carried out
 169 in duplicate obtaining reproducible results.

170 2.2. Calculation of BPA and polyurea (PU) yield

171 BPA yield was calculated through Eq. (2), where n_{BPA} are the moles of biphenol A
 172 isolated from the reaction mixture.

$$173 \text{ BPA yield (\%)} = (n_{BPA}/n^{\circ}_{BPA}) \times 100 \quad (2)$$

174 PU yield was calculated according to Eq. (3), where w_{PU} is the mass (g) of PU
 175 isolated and MM_{PU} is the molar mass of the PU repeating unit.

$$176 \text{ PU yield (\%)} = 100 \times (w_{PU} \times MM_{UR(PC)}) / (w \times MM_{PU}) \quad (3)$$

177 2.3. Determination of PC conversion

178 PC conversion in aminolysis experiments was determined spectrophotometrically by
 179 measuring in the FTIR spectrum of the reaction mixture the intensity of the residual
 180 absorption at 1778 cm^{-1} due to $\nu(\text{C}=\text{O})$ stretching in $-\text{OArOC}(\text{O})\text{OArO}-$ (Ar = 4,4'-
 181 $\text{C}_6\text{H}_4\text{CMe}_2\text{C}_6\text{H}_4-$) moieties of the starting polymer or its oligomers/fragments not completely
 182 depolymerized. The intensity of this signal was compared with the intensity of the
 183 absorption displayed, at the same wavenumber, by standard THF solutions of polycarbonate.
 184 PC conversion was, then, calculated through Eq. (4), wherein $w(\text{g})$ is the mass of feed PC

185 and $w_1(g)$ is the overall amount of polymer/oligomers not yet depolymerized and determined
186 spectrophotometrically by FTIR.

187
$$\text{PC conversion (\%)} = 100 \times (w - w_I) / w \quad (4)$$

188 *2.4. H₂NRNH₂ carbamation by PC diaminolysis (diamine/UR(PC) stoichiometric ratio: 0.5*
189 *mol/mol)*

190 As an example, we report the procedure followed with HMDA. The reaction was
191 carried out in a suitable glass tube (~40 mL) equipped with a Sovirel screw cap and a Torion
192 stopcock. The reactor, once charged with the reactants (PC, usually ~4 mmol_{UR(PC)}; HMDA,
193 1-1.14 equivalents; solvent (THF), usually 24 mL), was sealed and dipped into an
194 electrically heated silicon oil bath and the reaction mixture was stirred at the working
195 temperature until complete PC depolymerization, that was ascertained by monitoring the
196 disappearance of the polycarbonate absorption at 1778 cm⁻¹ in the FTIR spectrum of the
197 reaction mixture (Figs. S1a-S1c). Once PC conversion was complete, the reaction solution
198 was evaporated in vacuum and the residue was washed several times with diethyl ether. The
199 white solid insoluble in ether, once dried under vacuum, was analyzed by spectroscopic
200 methods (NMR and FTIR; Fig. S2a-S2c).

201 Depending on the reaction temperature (at 100 °C, for instance) minor amounts of a
202 colorless solid may separate from the reaction mixture. The FTIR spectrum of this material,
203 once isolated by filtration, showed bands typical of ureidic groups (see 3.1 and Fig. S1d).

204 *2.5. PC recycling by diaminolysis: BPA recovery and synthesis of PUs [-NHRNHCO-]_n*

205 The diaminolysis reaction was carried out in a reactor analogous to that described
206 above (2.4). In a typical experiment the reactor, once charged under an inert gas stream with
207 the reactants (PC; diamine (2 equivalents); solvent (THF); catalyst (DBU or NaOH), if
208 used), was sealed and dipped into an electrically heated silicon oil bath. The mixture was
209 stirred at the working temperature (120 °C) for a variable time, depending on the diamine

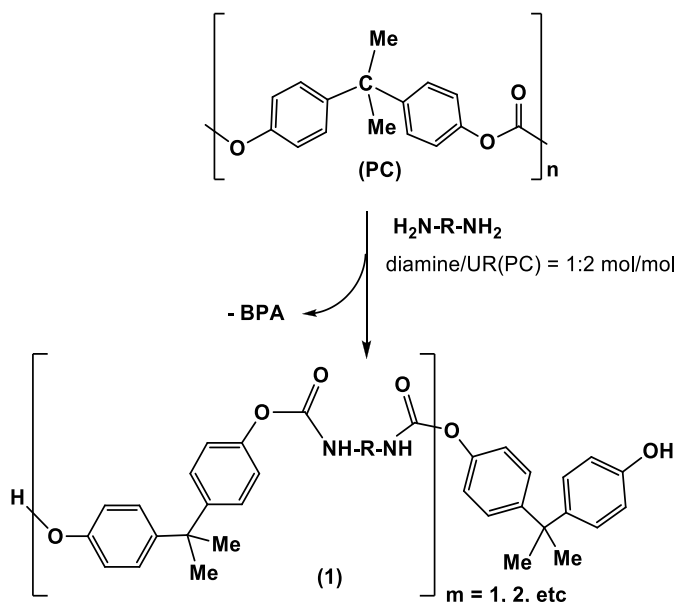
210 and the catalyst, if used (see 3.2 and Table 1 and 2). The solid precipitated was isolated by
 211 filtration and identified as polyurea, while BPA was recovered from the filtrate after
 212 removing THF. For further details see Tables 1 and 2, and Appendix A (Supplementary
 213 Data).

214 3. Results and discussion

215 Fig. 1 shows the diamines H_2NRNH_2 considered in this study. We have focused on
 216 industrially relevant diamines with a suitable spacer group R such as to prevent the
 217 undesired side-formation of cyclic ureas. The diaminolysis reaction was studied in THF, a
 218 solvent that easily dissolves PC as well as the diamines used.

219 3.1. H_2NRNH_2 carbamation by PC diaminolysis

220 The diaminolysis reaction was first studied using a 0.5 mol/mol diamine/UR(PC)
 221 stoichiometric ratio (diamine: 1 equivalent). This reaction was expected to afford urethane
 222 chains like **1**, besides BPA (Fig. 2). We selected an aliphatic diamine such as HMDA as the

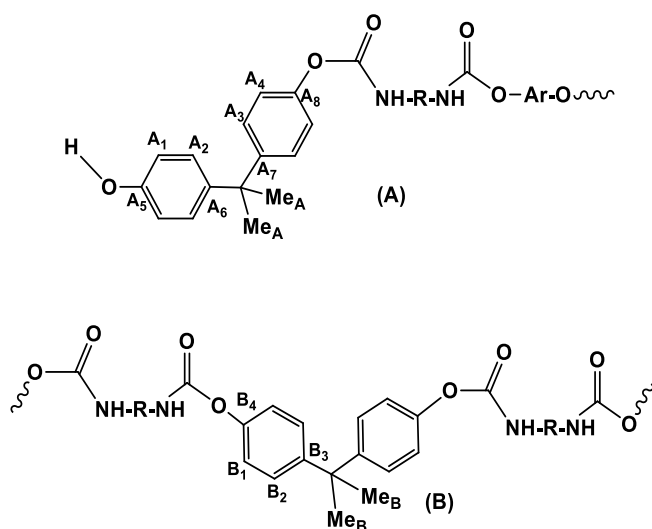


223

224 **Fig. 2.** PC diaminolysis (diamine/UR(PC) = 0.5 mol/mol): H_2NRNH_2 carbamation.

225 reference diamine. The progress of the reaction was monitored by following, in the IR
 226 spectrum of the reaction solution (Figs. S1a-c), the disappearance of the PC carbonyl
 227 absorption at 1778 cm^{-1} and the growth of the band at 1746 cm^{-1} due to $\nu(\text{C}=\text{O})$ carbamic
 228 stretching in urethanic species like **1** ($\text{R} = -(\text{CH}_2)_6-$) [Pan et al., 2015; Quaranta, 2017]. The
 229 formation of the latter species was accompanied by that of BPA, which is responsible for the
 230 signals observed at 1614 and 1591 cm^{-1} [Quaranta, 2017].

231 The urethane derivatives **1** ($\text{R} = -(\text{CH}_2)_6-$) cogenerated with BPA were isolated (see 2.4) and
 232 analyzed by FTIR and NMR spectroscopy. The IR spectrum shows the intense absorption of
 233 carbamate group at 1711 cm^{-1} (Fig. S2a) [Wu et al., 2018; Mattia and Painter, 2007; Distaso and
 234 Quaranta, 2004a; Aresta et al., 1998]. The aliphatic region of the ^1H NMR spectrum (Fig. S2b)
 235 displays the resonances due to the methylene protons of bis-carbamated HMDA at 1.28 (br), 1.44
 236 (br), 3.03 ppm (br) [Distaso and Quaranta, 2006]; accordingly, a broad resonance is also present at
 237 7.68 ppm that can be assigned to the carbamic NH protons. The absence of any methylene CH_2NH_2
 238 resonance around 2.6 ppm allows to exclude the presence of chains ending with free NH_2 groups,
 239 while the OH singlet at 9.17 ppm is consistent with the presence of urethanic chains **1** ($\text{R} = -(\text{CH}_2)_6-$
 240) bearing terminal $-\text{OArOH}$ ($\text{Ar} = 4,4'\text{-C}_6\text{H}_4\text{CMe}_2\text{C}_6\text{H}_4-$) groups **A** (Fig. 3), which are also
 241 responsible for the signals at 7.16 (m), 6.97 (m), 6.64 (d, $^3J_{\text{HH}} = 8.8\text{ Hz}$) and 1.56 ppm (s); the



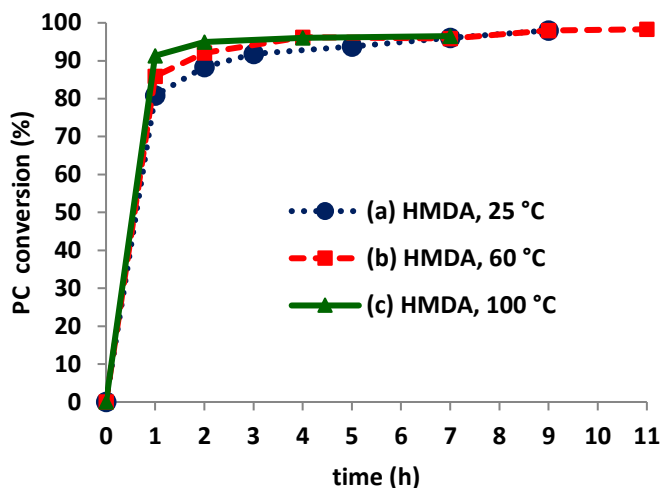
242

243 **Fig. 3.** Atom numbering in terminal $-\text{OArOH}$ groups **A** and inner $-\text{OArO}-$ groups **B**.

244 signals at 7.16 and 6.97 ppm are also due to inner -OArO- moieties **B** (Fig. 3), as well as the singlet
245 at 1.61 ppm. The analysis of the integral spectrum allows to calculate the molar ratio between
246 terminal -OArOH groups **A** and inner -OArO- groups **B**, which is ~1.5 mol/mol, as well as the
247 number average molecular weight M_n that was found to be close to 1200 Da. The inspection of the
248 ^{13}C -NMR spectrum (Fig. S2c) further supports the partial depolymerization of the
249 polycarbonate with the incorporation of the diamine in the PC framework and the formation
250 of **1** ($\text{R} = -(\text{CH}_2)_6-$).

251 The carbamation reaction proceeded without any auxiliary catalyst under very mild
252 conditions (25-60 °C) with practically quantitative PC conversion ($\geq 98\%$ after 9 h; Fig. 4, curve (a)
253 and (b)) and selectively, without any evidence of formation of ureidic derivatives. Accordingly, the
254 IR spectrum of the reaction mixture, that kept homogeneous throughout the reaction time (no
255 formation of precipitate), did not show, in the relevant range 1700-1620 cm^{-1} , any significant
256 absorption which might be diagnostic of the presence of ureidic species (free or associated) in
257 solution [Mido, 1973; Lortie et al., 2003]. Under the working conditions (Fig. 4, curve (a)
258 and (b)), the conversion rate, while being satisfactory soon after mixing the reactants, with
259 PC conversion higher than 80% after 1 h, slowed down a lot in the long run and the full
260 conversion of the polycarbonate required a markedly longer time. This behavior can be
261 obviously related to the lower and lower concentration of the reactants in the reaction
262 mixture, but may also reflect the fact that the aminolysis of organic carbonates is usually
263 promoted by amine itself, since a second molecule of amine can act as the catalyst of the
264 carbamation process [Carafa and Quaranta, 2009; Um et al., 2018]. This accounts for the
265 modest excess of diamine (max. 13 mol% relative to UR(PC)) usually used in the
266 carbamation experiments.

267 At 100 °C (Fig. 4, curve (c)) the conversion of PC was faster, but, at this temperature,
268 under the working conditions, minor amounts of a poorly soluble colorless solid separated



269

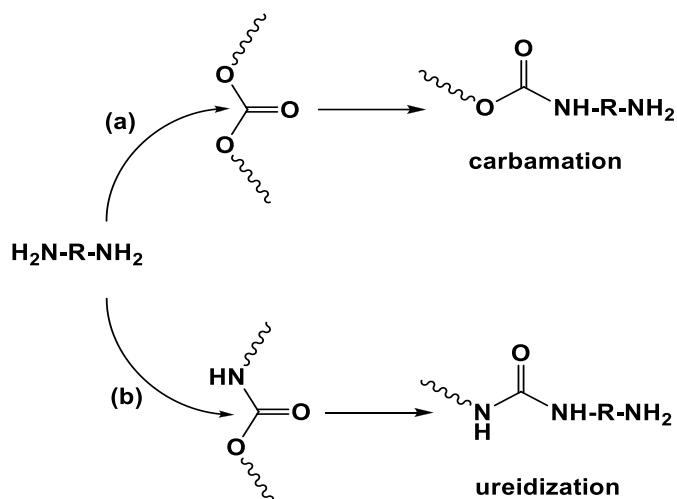
270 **Fig. 4.** HMDA carbamation by PC diaminolysis at different temperatures, in THF (24 mL).
 271 Experimental conditions: (a) UR(PC), 4.28 mmol; HMDA, 2.40 mmol; 25 °C. (b) UR(PC), 3.99
 272 mmol; HMDA, 2.26 mmol; 60 °C. (c) UR(PC), 4.23 mmol; HMDA, 2.38 mmol; 100 °C.

273

274 with time from the reaction mixture. In the FTIR spectrum of this material (Fig. S1d) two
 275 characteristic bands at 1614 (m-s) and 1576 cm^{-1} (m-s), assignable to ureidic moieties
 276 [Mido, 1972; Aresta et al., 1998] (see also 3.2.1), can be easily recognized among the other
 277 absorptions, showing that a concurrent ureidization reaction can occur at 100 °C in addition
 278 to the carbamation process.¹ As illustrated in Fig. 5, the ureidization reaction can compete
 279 with carbamation for the functionalization of the NH_2 groups and this, in the absence of a
 280 suitable excess of diamine, can prevent the conversion of the $-\text{OC}(\text{O})\text{O}-$ carbonate groups
 281 from being quantitative. Accordingly, in the experiment (c) of Fig. 4 PC conversion did not
 282 exceed 97% even after prolonged heating (7 h) at the working temperature (100 °C).

283 The study was extended to TOTDA and *m*-XYLDA. Both the diamines reacted with
 284 PC likewise HMDA to give urethane derivatives **1** ($\text{R} = -(\text{CH}_2)_3\text{O}(\text{CH}_2)_2\text{O}(\text{CH}_2)_2\text{O}(\text{CH}_2)_3-$;
 285 *m*- $\text{CH}_2\text{C}_6\text{H}_4\text{CH}_2-$; $\nu(\text{C}=\text{O})$: $\sim 1746 \text{ cm}^{-1}$, in THF solution). At ambient temperature (25 °C),

¹ Apart from the absorptions at 1614 and 1576 cm^{-1} , the FTIR spectrum of the solid precipitated (Fig. S1d) showed strong similarities with that of **1** ($\text{R} = -(\text{CH}_2)_6-$; Fig. S2a), suggesting the precipitation, under the working conditions, of ureidic-urethanic species.



286

287

Fig. 5. PC diaminolysis: carbamation versus ureidization.

288

289

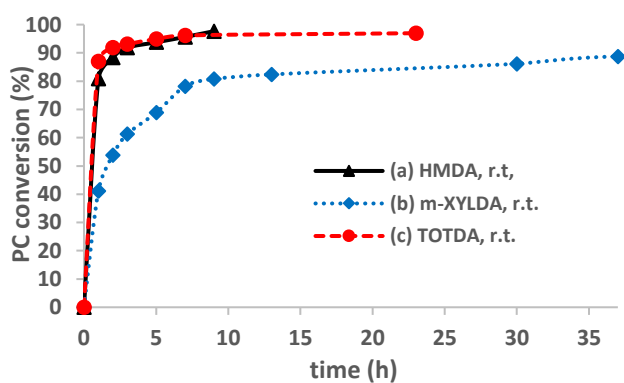
290

291

292

293

under conditions analogous to those used for HMDA, the carbamation of TOTDA and *m*-XYLDA proceeded homogeneously with very high selectivity without any evidence of formation of ureidic species (no absorptions between 1700 and 1620 cm^{-1} ; Fig. S3 and S4). Fig. 6 allows to compare, from the kinetic point of view, the behavior of HMDA, TOTDA and *m*-XYLDA as depolymerizing agents of the polycarbonate at ambient temperature. The kinetic curves support the following order of reactivity: TOTDA \cong HMDA > *m*-XYLDA.



294

295

296

297

298

299

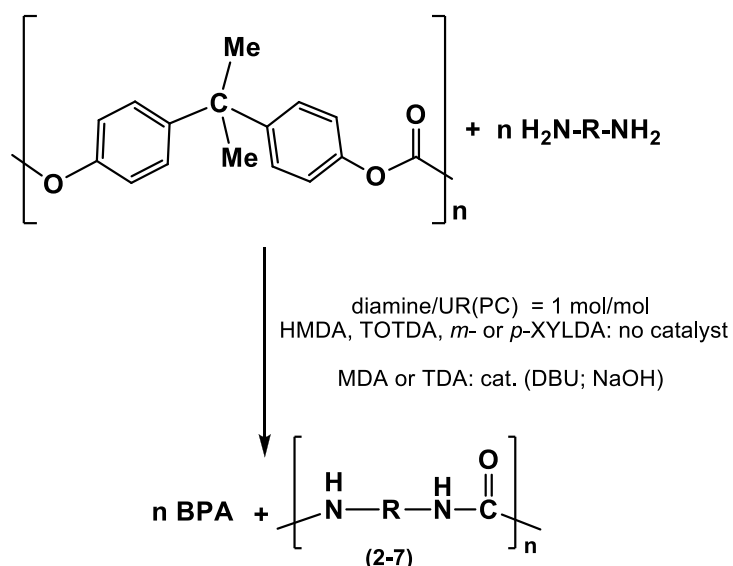
Fig. 6. Carbamation of HMDA (a), *m*-XYLDA (b) and TOTDA (c) by PC diaminolysis at room temperature (25 °C). (a) UR(PC), 4.28 mmol; HMDA, 2.40 mmol; THF, 24 mL. (b) UR(PC), 3.99 mmol; *m*-XYLDA, 2.27 mmol; THF, 24 mL. (c) UR(PC), 2.07 mmol; TOTDA, 1.14 mmol; THF, 12 mL.

300 In the absence of any catalyst, the aromatic diamine MDA did not react with PC
301 under conditions analogous to those described above for the basic diamines HMDA,
302 TOTDA and *m*-XYLDA. This behavior is not unexpected in view of the lower
303 nucleophilicity of aromatic versus aliphatic amines and is reminiscent of the poor reactivity
304 exhibited by MDA (as well as TDA) with diphenyl carbonate and other carbonic acid
305 diesters in the absence of any catalyst [Aresta et al., 1995; Aresta et al., 1999; Distaso and
306 Quaranta, 2004b].

307 3.2. Poly-(bisphenol A carbonate) recycling by diaminolysis: synthesis of polyureas

308 The above experiments suggest that relatively high temperatures can lower the selectivity of
309 the urethanization process (Fig. 2) and promote the ureidization reaction (Fig. 5, (b)). Such a
310 reactivity has been exploited from the synthetic standpoint with a view to providing a new synthetic
311 entry into non-isocyanate homo-polyureas using PC as the source of the carbonyl group (Fig. 7). To
312 this end the diamine/UR(PC) stoichiometric ratio was suitably changed and H₂NRNH₂ (2
313 equivalents) was reacted according to an equimolar ratio relative to the repeating unit of the
314 polymer. Also in this case THF was selected as the solvent of the aminolysis process.

315 Table 1 summarizes the results obtained at 120 °C when using the basic diamines HMDA,
316 TOTDA, *m*-XYLDA and *p*-XYLDA. Under the working conditions the conversion of the
317 polymer into BPA and the relevant polyureas (HMDA-PU, TOTDA-PU, *m*-XYLDA-PU and *p*-
318 XYLDA-PU, respectively) proceeded smoothly, within reasonable times that, however, may vary
319 sensibly with the used diamine. At the working temperature HMDA-PU, *m*-XYLDA-PU and *p*-
320 XYLDA-PU were poorly soluble in the reaction medium and separated as colorless solids. Under
321 analogous conditions TOTDA reacted likewise HMDA, *m*-XYLDA and *p*-XYLDA, but, in the
322 latter case, the aminolysis reaction proceeded homogeneously as the relevant polyurea (TOTDA-
323 PU) was soluble in the reaction solvent at the working temperature (120 °C). The precipitation of



| $\text{H}_2\text{N-R-NH}_2$ | $[-\text{NH-R-NHC(O)}-]_n$ | |
|-----------------------------|----------------------------|--|
| HMDA | HMDA-PU (2) | R = $-(\text{CH}_2)_6-$ |
| TOTDA | TOTDA-PU (3) | R = $-(\text{CH}_2)_3\text{O}(\text{CH}_2)_2\text{O}(\text{CH}_2)_2\text{O}(\text{CH}_2)_3-$ |
| <i>m</i> -XYLDA | <i>m</i> -XYLDA-PU (4) | R = <i>m</i> - $\text{CH}_2\text{C}_6\text{H}_4\text{CH}_2-$ |
| <i>p</i> -XYLDA | <i>p</i> -XYLDA-PU (5) | R = <i>p</i> - $\text{CH}_2\text{C}_6\text{H}_4\text{CH}_2-$ |
| MDA | MDA-PU (6) | R = 4,4'- $\text{C}_6\text{H}_4\text{CH}_2\text{C}_6\text{H}_4-$ |
| TDA | TDA-PU (7) | R = 2,4- $\text{C}_6\text{H}_3\text{Me}-$ |

324

325 **Fig. 7.** PC recycling by diaminolysis: synthesis of polyureas.

326

Table 1

PC depolymerization with the basic diamines HMDA, TOTDA, *m*-XYLDA and *p*-XYLDA (diamine/UR(PC) \cong 1 mol/mol) at 120 °C: synthesis of homo-polyureas.

| diamine (mmol) | UR(PC) (mmol) | THF (mL) | time (h) ^a | BPA (%) ^b | PU (%) ^b |
|------------------------|---------------|----------|-----------------------|----------------------|-------------------------|
| HMDA (4.62) | 4.05 | 15 | 2 | 83 | HMDA-PU (96) |
| TOTDA (4.56) | 4.00 | 15 | 2 | 85 | TOTDA-PU (78) |
| <i>m</i> -XYLDA (4.55) | 3.94 | 15 | 3.5 | 86 | <i>m</i> -XYLDA-PU (94) |
| <i>p</i> -XYLDA (2.26) | 1.93 | 7.5 | 12 | 83 | <i>p</i> -XYLDA-PU (99) |

^a Overall reaction time. At this time the depolymerization of PC was quantitative: the IR absorption at $\sim 1745 \text{ cm}^{-1}$ (due to intermediate urethanic species **1**, see 3.1) was no longer visible in the FTIR spectrum of the reaction mixture.

^b Isolated yield.

327

328 TOTDA-PU was observed only upon cooling the reaction mixture to room temperature.² In all the
329 cases BPA formed selectively without any significant formation of decomposition products (PhOH;
330 4-isopropenylphenol; 4-isopropylphenol) [Quaranta, 2017].

331 The process can be easily followed by FTIR spectroscopy (Figs. S5-S8). The
332 depolymerization of the polycarbonate goes through a carbamation step affording BPA and
333 urethane intermediates $\text{H}[-\text{OArOC}(\text{O})\text{NHRNHC}(\text{O})-]_n\text{OArOH}$ ($\text{Ar} = 4,4'\text{-C}_6\text{H}_4\text{C}(\text{Me})_2\text{C}_6\text{H}_4$ -
334), that, in a subsequent step, convert into $[-\text{NHRNHC}(\text{O})-]_n$ and more BPA. This reaction
335 sequence is well documented in Figs. S5-S8 for the ureidization of HMDA, TOTDA, *m*-
336 XYLDA an *p*-XYLDA, respectively. The intermediate formation of the urethane derivatives
337 **1** is unambiguously supported in the FTIR spectrum of the reaction mixture by the
338 appearance of the absorption at about 1745 cm^{-1} (see 3.1); the latter absorption disappeared
339 with time because of conversion of the carbamate intermediates $\text{H}[-$
340 $\text{OArOC}(\text{O})\text{NHRNHC}(\text{O})-]_n\text{OArOH}$ into the target PUs. It is worth noting that the IR
341 spectrum of the reaction solution (Figs. S5-S8) did not show any significant absorption in
342 the range $2275\text{-}2240\text{ cm}^{-1}$, where isocyanate group strongly absorbs. This brings to exclude
343 that the building up of the ureidic group might imply the amination of isocyanate
344 intermediates formed *in situ* from **1**. More likely, the formation of the $-\text{NHC}(\text{O})\text{NH}$ -
345 moieties involves the direct attack of free NH_2 to the carbamic groups of **1**.

346 PC depolymerization by the aromatic diamine MDA required conditions somewhat
347 different from those used with the basic diamines above considered. In fact, no reaction was
348 observed after 6 h at $120\text{ }^\circ\text{C}$ (entry 1, Table 2). The reaction was therefore investigated in
349 the presence of a base catalyst such as DBU. In the presence of DBU, MDA reacted very
350 slowly with PC at ambient temperature (Entry 2, Table 2). A faster reaction was observed at

351

² The FTIR spectrum of the liquid phase (Fig. S6), after cooling the reaction mixture at ambient temperature, showed characteristic absorptions at 1684 and 1653 cm^{-1} , respectively assigned to free and associated $\text{C}=\text{O}$ groups in ureidic oligomers [Mattia and Painter, 2007; Lortie et al., 2003; Mido, 1973].

Table 2

PC depolymerization with MDA or TDA (diamine/UR(PC) \cong 1 mol/mol): synthesis of homo-polyureas MDA-PU and TDA-PU.^a

| Entry | diamine (mmol) | UR(1) (mmol) | THF (mL) | T (°C) | catalyst (mol%) ^b | time (h) ^c | BPA (%) ^d | PU (%) ^d |
|-------|----------------|-----------------------|----------|--------|------------------------------|-----------------------|----------------------|---------------------|
| 1 | MDA (2.57) | 2.21 | 25 | 120 | - | 6 | ^e | ^e |
| 2 | MDA (2.61) | 2.26 | 25 | 25 | DBU (10.0) | 64 | ^f | - |
| 3 | MDA (2.59) | 2.23 | 25 | 120 | DBU (10.5) | 27 | 83 | MDA-PU (94) |
| 4 | MDA (2.43) | 2.06 | 25 | 120 | DBU (20.3) | 20 | 84 | MDA-PU (93) |
| 5 | MDA (3.09) | 2.59 | 30 | 120 | NaOH (15.3) | 6 | 86 | MDA-PU (89) |
| 6 | MDA (3.46) | 2.99 | 20 | 120 | NaOH (15.7) | 6 | 84 ^g | MDA-PU (88) |
| 7 | TDA (5.69) | 4.83 | 30 | 120 | NaOH (14.0) | 7 | 95 | TDA-PU (87) |

^a PC depolymerization by diamines MDA or TDA was followed by FTIR analysis of the THF solution, by monitoring over time the absorptions at 1778 cm⁻¹ (due to PC) and 1715-1717 cm⁻¹ (due to **1**; R = 4,4'-C₆H₄CH₂C₆H₄- or 2,4-C₆H₃Me, according to the used diamine (MDA or TDA)). See also 3.2 and Figs. S9 and S10.

^b mol% relative to UR(PC).

^c Overall reaction time.

^d Isolated yield.

^e No reaction.

^f Only traces amounts of BPA were detected in the reaction mixture.

^g Isolated by column chromatography (see Supplementary Material).

352

353 120 °C: the progress of the reaction, monitored by FTIR spectroscopy (Fig. S9), was
 354 demonstrated by the decrease over time of the bands at 1778 and 1630 cm⁻¹, respectively due
 355 to PC and MDA, by the temporary appearance of the absorption at 1717 cm⁻¹, due to ν (C=O) of
 356 the urethanic intermediates **1** (R = 4,4'-C₆H₄CH₂C₆H₄-), by the growth of the bands at 1614 and
 357 1593 cm⁻¹ (BPA), and, finally, by the precipitation of a colorless solid isolated and characterized as
 358 MDA-PU. Nevertheless, the disappearance of the bands at 1778 cm⁻¹ (PC) and 1717 cm⁻¹ (**1**; R =
 359 4,4'-C₆H₄CH₂C₆H₄-) still required quite a long reaction time that depended on the DBU load (Entry

360 3 and 4, Table 2). The attention was, therefore, addressed to a different more effective base catalyst
361 such as NaOH. Remarkably, a significant shortening of the depolymerization time was attained by
362 using NaOH (15 mol%) as the catalyst of the aminolysis process (Entry 5 and 6, Table 2) in place of
363 the amidine base. The latter catalyst was, therefore, preferred for the ureidization of TDA. In the
364 presence of the alkali catalyst also TDA reacted effectively with PC, likewise MDA, to give the
365 relevant polyurea TDA-PU in addition to BPA (Entry 7, Table 2).

366 As a whole, the above results show that PU formation by PC diaminolysis can take
367 place quite easily under non severe conditions. The developed protocol stands out for the
368 modest excess of the used diamine substrate relative to the polymer (in most cases ~15
369 mol% versus the stoichiometric amount (diamine/UR(PC) = 1 mol/mol)). Moreover, basic
370 diamines react with PC in the absence of any auxiliary catalyst. Actually, diamine itself can
371 act, in principle, as the catalyst of the overall process (Fig. 7), in virtue of the well-known
372 ability of basic amines to promote catalytically not only the aminolysis reaction of organic
373 carbonates to carbamates [Carafa and Quaranta, 2009; Um et al., 2018] but also the
374 aminolysis of carbamic esters to ureas [Shawali et al., 1986]. The assistance of a catalyst is
375 required when using poorly nucleophilic amines. In this case the best results have been
376 obtained with a commercially accessible and cheap catalyst, such as NaOH. The latter issue is
377 not trifling as inexpensiveness is expected to be a key feature of any waste valorization process that
378 aims at having applicative potential.

379 3.2.1. Spectroscopic characterization of the polyureas

380 The polyureas **2-7** (Fig. 7) can be isolated straightforwardly with high yield (Table 1 and 2)
381 by filtration, once the reaction mixture was cooled to room temperature. Also BPA can be easily
382 recovered in good yield according to conventional techniques (see Supplementary Material).

383 All the PUs have been characterized spectroscopically in the solid state by ATR (Figs. S11a-
384 f), FTIR (in nujol mull; Figs. S12a-f) and CP/MAS ¹³C NMR (Figs. S13a-f).

385 As a whole, the IR spectra of the isolated PUs are in excellent accordance with those
 386 reported in the literature for authentic samples of analogue polyureas prepared by different synthetic
 387 routes (Table 3). For HMDA-PU, TOTDA-PU, *m*-XYLDA-PU and *p*-XYLDA-PU the amide II
 388 band (OCN-H) can be located between 1570 and 1591 cm^{-1} , while the amide I band ($\nu(\text{C}=\text{O})$) and

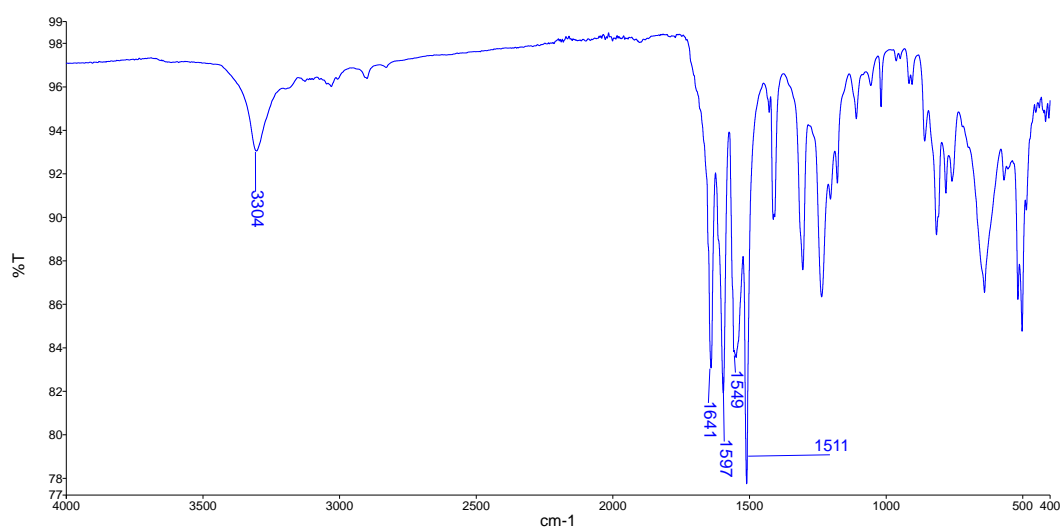
Table 3

FTIR (in nujol mull) and ATR characteristic bands (cm^{-1}) of the isolated PUs.

| PU | $\nu(\text{N-H})$ | amide I | amide II | Refs. |
|--------------------|-------------------|------------|------------|--|
| | ATR; FTIR | ATR; FTIR | ATR; FTIR | |
| HMDA-PU | 3330; 3329 | 1616; 1618 | 1575; 1580 | [Shang et al., 2012; Wu et al., 2012; Wang et al., 2016] |
| TOTDA-PU | 3318; 3319 | 1611; 1614 | 1587; 1591 | [Ying et al., 2015] |
| <i>m</i> -XYLDA-PU | 3315; 3316 | 1622; 1622 | 1579; 1584 | [Wu et al., 2012] |
| <i>p</i> -XYLDA-PU | 3318; 3319 | 1614; 1614 | 1570; 1574 | [Wu et al., 2012] |
| MDA-PU | 3304; 3304 | 1641; 1641 | 1549; 1545 | [Rockicki, 1988] |
| TDA-PU | 3264; 3285 | 1637; 1639 | 1538; 1545 | [Han et al., 2014; Li et al., 2015] |

389

390 the N-H stretching ($\nu(\text{N-H})$) are respectively found in the ranges 1611-1622 and 3315-3330 cm^{-1}
 391 (Table 3). In the spectrum of MDA-PU (Fig. 8) and TDA-PU the above absorptions are shifted in

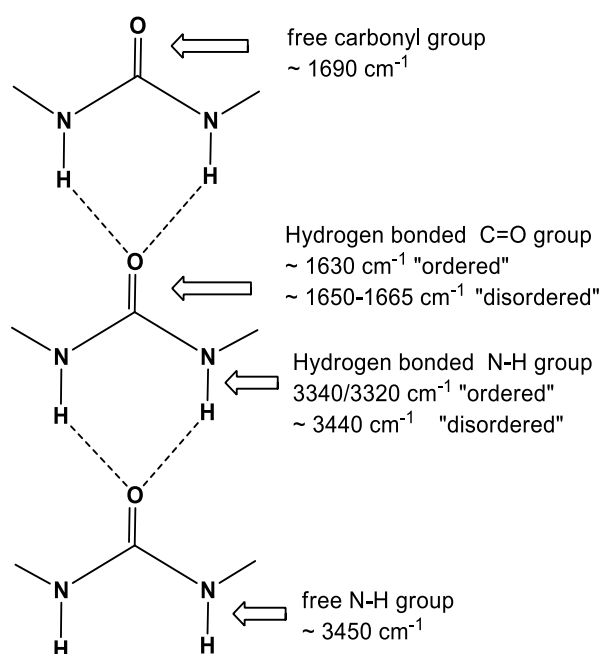


392

393 **Fig. 8.** ATR-FTIR spectrum of MDA-PU: IR: $\nu = 3304$ (NH), 1641 (amide I), 1597, 1549 (amide
 394 II), 1511, cm^{-1} .

395

396 accordance with the aromatic nature of the diamine used (MDA and TDA, respectively) [Socrates,
 397 2001]. In any case the location of the IR bands due to $\nu(\text{C}=\text{O})$ and $\nu(\text{N}-\text{H})$ is very informative as it
 398 supports that the carbonyl oxygen atoms and the N-H groups are involved in a strong H-bond
 399 (Fig. 9) [Li et al., 2015; He et al., 2014; Yilgor et. al., 2000; Coleman et al., 1997]. In fact, both
 400 $\nu(\text{N}-\text{H})$ and $\nu(\text{C}=\text{O})$ are markedly red-shifted relative to the frequency of free N-H (3450 cm^{-1}) and
 401 free C=O (1690 cm^{-1}) groups in polyureas. Moreover, the positions of $\nu(\text{N}-\text{H})$ and $\nu(\text{C}=\text{O})$ are
 402 typical of "hydrogen-bonded ordered" bands suggesting the presence of hydrogen-bonded groups in
 403 network structures characterized by some degree of order or regularity (Fig. 9). This may explain
 404 the high resistance of the isolated materials to common organic solvents such as hydrocarbons,
 405 aromatics, THF, diethyl ether, acetone, acetonitrile, DMF, methanol, 2-propanol. Table 4 compares
 406 the behavior of the isolated PUs in a few other solvents such as H_2O , CHCl_3 , DMSO.



408 **Fig. 9.** Hydrogen bondings in polyureas (from ref. [Mattia and Painter, 2007]).

409 The polyureidic nature of the isolated products **2-7** (Fig. 7) is further supported by solid state
 410 CP/MAS ^{13}C NMR measurements (Fig. S13a-S13f and Table 5). In most cases the resonance of the
 411 ureidic carbons can be located around 160 ppm in strict accordance with the literature. In the
 412 CP/MAS ^{13}C NMR spectrum of MDA-PU (Fig. 10) the C=O resonance was found at higher field,

413 151.9 ppm, in accordance with the calculated value of 152.2 ppm and the experimental value (~152
 414 ppm) found for a structurally related ureidic derivative of MDA [Aresta et al., 1998].

Table 4

Solubility behavior of the isolated PUs in a few solvents at ambient temperature (22 °C).

| Solvent | HMDA-PU | TOTDA-PU | <i>m</i> -XYLDA-PU | <i>p</i> -XYLDA-PU | MDA-PU | TDA-PU |
|-------------------|---------|----------|--------------------|--------------------|--------|--------|
| H ₂ O | - | + | - | - | - | - |
| CHCl ₃ | - | + | - | - | - | - |
| DMSO | - | - | - | - | - | + |

“-”: insoluble.

“+”: soluble.

415

Table 5

CP/MAS ¹³C NMR data ($\delta_{C=O}$, ppm) for the isolated polyureas.

| PU | HMDA-PU | TOTDA-PU | <i>m</i> -XYLDA-PU | <i>p</i> -XYLDA-PU | MDA-PU | TDA-PU |
|----------------|--------------------|--------------------|--------------------|--------------------|----------------------|--------|
| $\delta_{C=O}$ | 160.7 ^a | 160.0 ^b | 160.0 ^c | 159.0 ^c | 151.9 ^{d,e} | 157.7 |

^a See also refs [Shang et al., 2012] and [Wu et al., 2012].

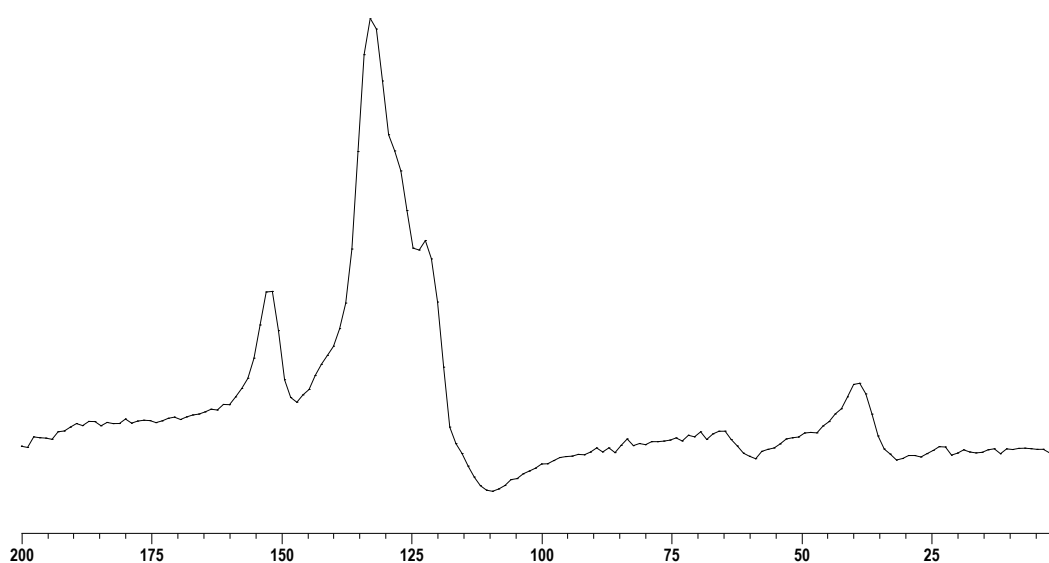
^b See also ref. [Ying et al., 2015].

^c See also ref. [Wu et al., 2012].

^d Calculated: 152.2 ppm (software: ACD/C+H NMR Predictors and DB (v.12.01)).

^e See also ref. [Aresta et al., 1998].

416



417

418 **Fig. 10.** CP/MAS ¹³C-NMR (151 MHz) of MDA-PU: δ = 39.0 (CH₂), 121.3-133.1 (aromatic
 419 carbons), 151.9 (C=O) ppm.

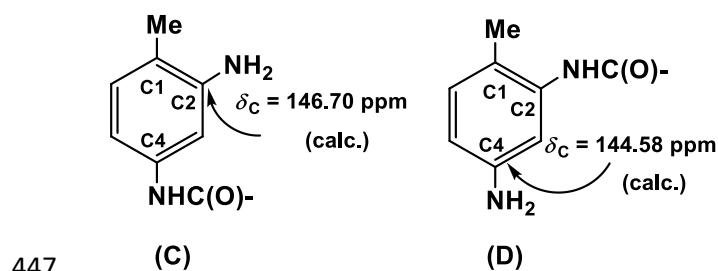
420

421 The insolubility in common organic solvents has prevented, for most of the PUs synthesized,
422 any attempt of determination of molecular weights by means of traditional techniques. However,
423 because of their solubility properties (Table 4), it was possible to characterize polyureas TOTDA-
424 PU and TDA-PU by NMR spectroscopy also in solution. The NMR analysis confirmed the
425 polyureidic nature of these products, demonstrated their homogeneity, and, by means of end-group
426 analysis, allowed to estimate the degree of polymerization, providing thus a further validation of the
427 developed synthetic approaches.

428 Figs. S14 and S15 illustrate, respectively, the ^1H and ^{13}C NMR of TOTDA-PU in D_2O . The
429 ^{13}C NMR spectrum shows all the signals of the repeating unit of the polyurea. The ^1H spectrum
430 displays also additional distinguishable resonances assignable to $\text{H}_2\text{NRNHCO-}$ end groups. The
431 integral proton spectrum allows to determine the number average molecular weight of TOTDA-PU
432 ($M_n = 2553$ Da) and to calculate the average number of repeating monomer units ($n = 9.5$).

433 The ^1H and ^{13}C NMR spectra of TDA-PU in DMSO-d_6 are reported in Figs. S16 and
434 S17, respectively. The integrals of the signals due to the NH_2 protons of the terminal TDA
435 moieties and those of all the methyl protons allow to evaluate the number of [2,4-
436 $\text{NHC}_6\text{H}_3\text{Me-NHCO-}$] repeating units ($n = 9.6$) and calculate M_n (1544 Da). In the ^{13}C NMR
437 spectrum of TDA-PU two very close resonances are found for the carbonyl carbons (152.73
438 and 152.42 ppm) that, therefore, in DMSO solution resonate at higher fields than in the solid
439 state (157.7 ppm). The analysis of the ^{13}C NMR spectrum allows to shed light on the nature
440 of the terminal group of the polymeric chains and identifies as **C** the most likely structure
441 for the end groups of the polyureidic chains (Fig. 11). This agrees well with the fact that the
442 two amino groups of TDA, that, differently from those of the other diamines considered in
443 this study, are not equivalent, exhibit a different reactivity for steric reasons, so the 4- NH_2
444 group is carbonylated more easily than that in *ortho* position to the methyl group [Aresta et
445 al., 1998; Distaso and Quaranta, 2004b].

446



448 **Fig. 11.** Possible isomeric end-groups for TDA-PU. The carbon atom directly bound to the NH_2
 449 group, C2 in (C) and C4 in (D), has been selected as suitable probe to distinguish between the
 450 two isomeric structures: the relevant ^{13}C nuclei, in fact, are expected to resonate at different
 451 δ_C (146.70 and 144.58 ppm; calculated with the software ACD/C+H NMR Predictors and DB
 452 (v.12.01)). For a more detailed discussion, see Supplementary Material (Fig. S17).

453 3.2.2. Thermal properties of the polyureas

454 The thermal properties of PUs **2-7** (Fig. 7) have been assessed by DSC and TGA. The
 455 second heating DSC curves are shown in Fig. 12 (left side). Only TOTDA-PU exhibits a melting
 456 behavior in the range 0-200 °C owing to the presence of ether moieties that make the polyurea
 457 structure very flexible [Dennis et al., 2018] and lower the melting temperature. The bimodal
 458 structure of the melting signals at 85.2 °C and 107.3 °C, also evident in the first heating run, is
 459 associated to different populations of lamellar crystals [Ying et al., 2015] and due to melting-
 460 recrystallization-melting phenomena [Jiang et al., 2019].³

461 The DSC curves of the other PUs show the presence of glass transitions associated to the
 462 amorphous portion of the solids. The T_g value of HMDA-PU is 54.5 °C, that falls in the T_g range 44
 463 °C - 74 °C characteristic of polyureas with similar structure [Shang et al., 2012; Kébir et al., 2017].
 464 *m*-XYLDA-PU undergoes glass transition at 42.4 °C, while the more symmetrical polyurea *p*-
 465 XYLDA-PU has a higher T_g value (77.6 °C). TDA-PU and MDA-PU show glass transition at 69.0
 466 °C and 135.5 °C, respectively.

467 Inspection of the TGA plots, Fig. 12 (right side), performed by differential weight loss
 468 (curves not shown), reveals that only PUs TOTDA-PU and TDA-PU decomposed in one step,

³ Only a crystallization exothermic peak at 60.2 °C was observed during the cooling run (not shown).

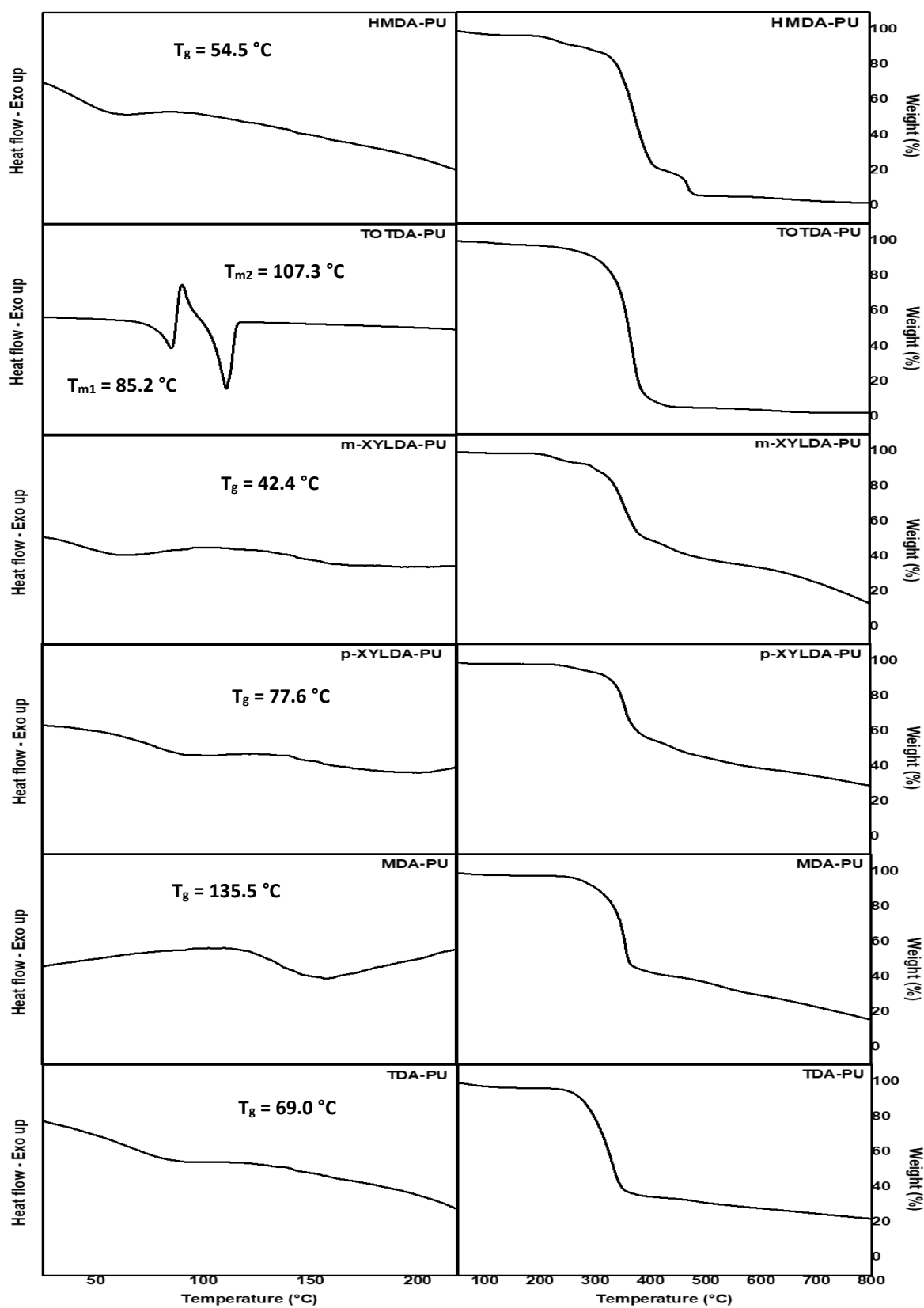


Fig. 12. DSC (left side) and TGA (right side) curves of the isolated PUs. The reported DSC curves were obtained from the second heating scan.

501 whereas all the other PUs showed a multi-stage decomposition process. The temperatures that
 502 characterize the process of thermal decomposition of all the isolated PUs are reported in Table 6.

Table 6

Thermal properties of the isolated PUs measured by TGA.^a

| PU | $T_{d,5\%}$ (°C) ^b | $T_{d,1/2}$ (°C) ^c | $T_{d,max}$ (°C) ^d | $M_{residue}$ (%) ^e |
|--------------------|-------------------------------|-------------------------------|-------------------------------|--------------------------------|
| HMDA-PU | 212 | 368 | 366 | 2.8 |
| TOTDA-PU | 252 | 356 | 364 | 2.6 |
| <i>m</i> -XYLDA-PU | 235 | 390 | 347 | 25.1 |
| <i>p</i> -XYLDA-PU | 268 | 440 | 347 | 34.3 |
| MDA-PU | 270 | 355 | 349 | 22.8 |
| TDA-PU | 243 | 328 | 323 | 25.0 |

^a Heating rate: 10 °C/min.

^b Temperature at which weight loss is 5%.

^c Temperature at which weight loss is 50%.

^d Temperature at which the rate of decomposition is maximum.

^e Residual weight observed at 750 °C.

503

504 The thermal stability of polyureas increases with the monomer molecular weight [Kèbir et al, 2017]
 505 and depends on the polymer structure, in particular symmetry and rigidity [Esfahanizadeh et al.,
 506 2015]. The presence of more rigid aromatic units along the chain leads to a general increase of
 507 stability [Ban et al., 2019]. Accordingly, *m*-XYLDA-PU, *p*-XYLDA-PU, MDA-PU and TDA-PU
 508 have a higher $T_{d,5\%}$ than the aliphatic HMDA-PU. Moreover, MDA-PU, with two aromatic units
 509 per repeating unit, shows the highest $T_{d,5\%}$. It is worth noting that *p*-XYLDA-PU has a higher $T_{d,5\%}$
 510 than *m*-XYLDA-PU as a result of the more symmetric structure, but both polyureas *m*-XYLDA-PU
 511 and *p*-XYLDA-PU, having the same molecular formula, have the maximum rate of decomposition
 512 at the same temperature.

513 The char residue formed after complete evaporation of the evolved species is higher for *m*-
 514 XYLDA-PU, *p*-XYLDA-PU, MDA-PU and TDA-PU than for HMDA-PU and TOTDA-PU
 515 because the presence of aromatic units causes an increase of the graphitization extent at high
 516 temperature [Ban et al., 2019].

517 In summary, the thermogravimetric analysis indicates that the above PUs have high thermal
518 stability [Ying et al., 2015] since they are stable up to 212–270 °C depending on structure, and have
519 the maximum rate of decomposition in the range of 323–366 °C. These results are noteworthy from
520 the practical standpoint for their applicative potential and suggest that the isolated PUs are suitable
521 for being processed using conventional techniques since their degradation process begins at a
522 temperature about 100 °C higher than their glass transition or melting temperature.

523 4. Conclusions

524 The reaction of poly-(bisphenol A carbonate) with either aliphatic or aromatic long-
525 chain diamines has been explored as a way to regenerate the monomer BPA and, for the first
526 time, to afford polyureas. The study provides an unprecedented approach to the valorization
527 of potentially hazardous PC wastes by chemical recycling and opens a new carbon-saving
528 synthetic entry into homo-polyureas through a non-isocyanate route.

529 In THF, under non severe conditions (120 °C), basic diamines, such as HMDA,
530 TOTDA, *m*-XYLDA and *p*-XYLDA (2 equivalents), reacted with PC, without any auxiliary
531 catalyst, to afford BPA and the relevant homo-polyureas [-NHRNHCO-]_n (HMDA-PU,
532 TOTDA-PU, *m*-XYLDA-PU and *p*-XYLDA-PU, respectively). Under otherwise analogous
533 conditions, the conversion of the less reactive aromatic diamines MDA or TDA (2
534 equivalents) required the assistance of a base catalyst (NaOH, DBU).

535 Polyurea formation goes through a carbamation step affording BPA and intermediate
536 urethane derivatives H-[OArOCONHRNHCO]_n-OArOH (**1**) (Ar = 4,4'-C₆H₄CMe₂C₆H₄-),
537 that in a subsequent step convert into [-NHRNHCO-]_n products and more BPA.

538 The developed synthetic methodology is 100% atomically economic, operationally
539 easy, does not require any complex equipment, is characterized by high productivity and
540 selectivity. In all the cases the depolymerization of the polymer (PC) was quantitative. Both
541 BPA and polyureas can be isolated straightforwardly in high yield through conventional

542 techniques. The thermal properties ($T_{d,5\%}$, $T_{d,1/2}$, T_g , T_m) of HMDA-PU, TOTDA-PU, *m*-
543 XYLDA-PU, *p*-XYLDA-PU, MDA-PU and TDA-PU, measured by DSC and TGA, make
544 these materials suitable for being processed.

545

546 **Acknowledgements**

547 This work was supported by Università degli Studi di Bari “Aldo Moro” (Fondi di Ateneo).

548 LAMIPLAST SRL (Modugno, Bari) is gratefully acknowledged for a generous gift of PC.

549 Thanks are due to Dr. Damiano Sgherza for some experimental assistance.

550 **Conflict of interest**

551 The authors declare no conflict of interest.

552

553 **Appendix A (Supplementary Data)**

554 Supplementary material related to this article is available as a separate file.

555

556 **References**

- 557 Alberti, C., Kessler, J., Eckelt, S., Hofmann, M., Kindler, T.O., Santangelo, N., Fedorenko, E.
558 Enthaler, S., 2020a. Hydrogenative Depolymerization of End-of-Life Poly(bisphenol A carbonate)
559 with in situ Generated Ruthenium Catalysts. *ChemistrySelect* 5, 4231-4234.
560 <https://doi.org/10.1002/slct.202000626>.
- 561
- 562 Alberti, C., Enthaler, S., 2020b. Depolymerization of End-of-Life Poly(bisphenol A carbonate) via
563 Alkali-Metal-Halide-Catalyzed Methanolysis. *Asian J. Org. Chem.* 9, 359-363.
564 <https://doi.org/10.1002/ajoc.201900242>.
- 565
- 566 Alberti, C., Scheliga, F., Enthaler, S., 2019. Recycling of End-of-Life Poly(bisphenol A
567 carbonate) via Alkali Metal Halide-Catalyzed Phenolysis. *ChemistryOpen* 8, 822–827.
568 <https://doi.org/10.1002/open.201900149>.
- 569
- 570 Antonakou, E.V., Achilias, D.S., 2013. Recent advances in polycarbonate recycling: A review of
571 degradation methods and their mechanisms. *Waste Biomass Valori.* 4, 9-21.
572 <https://doi.org/10.1007/s12649-012-9159-x>.
- 573
- 574 Aresta, M., Berloco, C., Quaranta, E., 1995. Biomimetic building-up of the carbamic moiety: the
575 intermediacy of carboxyphosphate analogues in the synthesis of N-aryl carbamate esters from
576 arylamines and organic carbonates promoted by phosphorous acids. *Tetrahedron.* 51, 8073-8088.
577 [https://doi.org/10.1016/0040-4020\(95\)00424-7](https://doi.org/10.1016/0040-4020(95)00424-7).
- 578

- 579 Aresta, M., Dibenedetto, A., Quaranta, E., 1998. Reaction of aromatic diamines with diphenyl
580 carbonate catalyzed by phosphorous acids: a new clean synthetic route to mono- and dicarbamates.
581 *Tetrahedron*. 54, 14145-14156. [https://doi.org/10.1016/S0040-4020\(98\)00873-4](https://doi.org/10.1016/S0040-4020(98)00873-4).
582
- 583 Aresta, M., Dibenedetto, A., Quaranta, E., 1999. Selective carbomethoxylation of aromatic
584 diamines with mixed carbonic acid diesters in the presence of phosphorous acids. *Green Chem.* 1,
585 237-242. <https://doi.org/10.1039/A904624K>.
586
- 587 Asscoated Press News, 2018. <https://apnews.com/0251b75ab0de4d3080214e95a57bf0ee> (accessed
588 27 May 2020).
589
- 590 Ban, J., Li, S., Yi, C., Zhao, J., Zhang, Z., Zhang, J., 2019. Amorphous and Crystallizable
591 Thermoplastic Polyureas Synthesized through a One-pot Non-isocyanate Route. *Chin. J. Polym.*
592 *Sci.* 37, 43–51. <https://doi.org/10.1007/s10118-018-2165-0>.
593
- 594 Carafa, M., Quaranta, E., 2009. Synthesis of Organic Carbamates without Using Phosgene:
595 Carbonylation of Amines with Carbonic Acid Diesters. *Mini-Rev. Org. Chem.* 6, 168-183.
596 <https://doi.org/10.2174/157019309788922720>.
597
- 598 Coleman, M.M., Sobkowiak, M., Pehlert, G.J., Painter, P.C., Iqbal, T., 1997. Infrared temperature
599 studies of a simple polyurea. *Macromol. Chem. Phys.* 198, 117-136.
600 <https://doi.org/10.1002/macp.1997.021980110>.
601
- 602 Datta, J., Kopczynska, P., 2016. From polymer waste to potential main industrial products: Actual
603 state of recycling and recovering. *Crit. Rev. Environ. Sci. Technol.* 46, 905-946.
604 <https://doi.org/10.1080/10643389.2016.1180227>.

- 605 Demarteau, J., O’Harra, K.E., Bara, J.E., Sardon, H., 2020. Valorization of Plastic Wastes for the
606 Synthesis of Imidazolium-Based Self-Supported Elastomeric Ionenenes. *ChemSusChem* 13, 3122-
607 3126. <https://doi.org/10.1002/cssc.202000505>.
- 608
- 609 Dennis, J.M., Steinberg, L.I., Pekkanen, A.M., Maiz, J., Hegde, M., Muller, A.J., Long, T.E., 2018.
610 Synthesis and Characterization of Isocyanate-free Polyureas. *Green Chem.* 20, 243-249.
611 <https://doi.org/10.1039/C7GC02996A>.
- 612
- 613 Distaso, M., Quaranta, E., 2004a. Group 3 metal (Sc, La) triflates as catalysts for the
614 carbomethoxylation of aliphatic amines with dimethylcarbonate under mild conditions.
615 *Tetrahedron.* 60, 1531. <https://doi.org/10.1016/j.tet.2003.12.020>.
- 616
- 617 Distaso, M., Quaranta, E., 2004b. Carbomethoxylating reactivity of methyl phenyl carbonate toward
618 aromatic amines in the presence of group 3 metal (Sc, La) triflate catalyst. *J. Catal.* 228, 36-42.
619 <https://doi.org/10.1016/j.jcat.2004.08.004>.
- 620
- 621 Distaso, M., Quaranta, E., 2006. Highly selective carbamation of aliphatic diamines under mild
622 conditions using Sc(OTf)₃ as catalyst and dimethyl carbonate as a phosgene substitute. *Appl. Catal.*
623 *B Environ.* 66, 72-80. <https://doi.org/10.1016/j.apcatb.2006.02.019>.
- 624
- 625 Do, T., Baral, E.R., Kim, J.G., 2018. Chemical recycling of poly(bisphenol A carbonate): 1,5,7-
626 Triazabicyclo[4.4.0]-dec-5-ene catalyzed alcoholysis for highly efficient bisphenol A and organic
627 carbonate recovery. *Polymer.* 143, 106–114. <https://doi.org/10.1016/j.polymer.2018.04.015>.
- 628

- 629 Esfahanizadeh, M., Sabbaghian, E., Mehdipour-Ataei, S., Jalilian, S., Babanzadeh, S., 2015.
630 Synthesis and Characterization of New Polyureas with Improved Thermal Stability from a Novel
631 Ether Keto Diamine. *Adv. Polym. Technol.* 34, 21511. <https://doi.org/10.1002/adv.21511>.
632
- 633 Fortman, D.J., Brutman, J.P., De Hoe, G.X., Snyder, R.L., Dichtel, W.R., Hillmyer, M.A., 2018.
634 Approaches to Sustainable and Continually Recyclable Cross-Linked Polymers. *ACS Sustainable*
635 *Chem. Eng.* 6, 11145-11159. <https://doi.org/10.1021/acssuschemeng.8b02355>.
636
- 637 Han, H., Li, S., Zhu, X., Jiang, X., Kong, X.Z., 2014. One step preparation of porous polyurea by
638 reaction of toluene diisocyanate with water and its characterization. *RSC Adv.* 4, 33520–33529.
639 <https://doi.org/10.1039/C4RA06383J>.
640
- 641 Hata, S., Goto, H., Yamada, E., Oku, A., 2002. Chemical conversion of polycarbonate to 1,3-
642 dimethyl-2-imidazolidinone (DMI) and bisphenol A: a practical approach to the chemical recycling
643 of plastic wastes. *Polymer.* 43, 2109-2116. [https://doi.org/10.1016/S0032-3861\(01\)00800-X](https://doi.org/10.1016/S0032-3861(01)00800-X).
644
- 645 Hata, S., Goto, H., Tanaka, S., Oku, A., 2003. Viable Utilization of Polycarbonate as a Phosgene
646 Equivalent Illustrated by Reactions with Alkanedithiols, Mercaptoethanol, Aminoethanethiol, and
647 Aminoethanol: A Solution for the Issue of Carbon Resource Conservation. *J. Appl. Polym. Sci.* 90,
648 2959-2968. <https://doi.org/10.1002/app.12936>.
649
- 650 He, Y., Xie, D., Zhang, X., 2014. The structure, microphase-separated morphology, and property of
651 polyurethanes and polyureas. *J. Mater. Sci.* 49, 7339-7352. [https://doi.org/10.1007/s10853-014-](https://doi.org/10.1007/s10853-014-8458-y)
652 [8458-y](https://doi.org/10.1007/s10853-014-8458-y).
653

- 654 Hong, M., Chen, E.Y.-X., 2017. Chemically Recyclable Polymers: A Circular Economy Approach
655 to Sustainability. *Green Chem.* 19, 3692–3706. <https://doi.org/10.1039/C7GC01496A>.
656
- 657 Iannone, F., Casiello, M., Monopoli, A., Cotugno, P., Sportelli, M.C., Picca, R.A., Cioffi, N.,
658 Dell'Anna, M.M., Nacci, A., 2017. Ionic liquids/ZnO nanoparticles as recyclable catalyst for
659 polycarbonate depolymerization. *J. Mol. Catal. A Chem.* 426, 107-116.
660 <https://doi.org/10.1016/j.molcata.2016.11.006>.
661
- 662 Jehanno, C., Pérez-Madrigal, M.M., Demarteau, J., Sardon, H., Dove, A.P., 2019. Organocatalysis
663 for depolymerisation. *Polym. Chem.* 10, 172-186. <https://doi.org/10.1039/C8PY01284A>.
664
- 665 Jehanno, C., Demarteau, J., Mantione, D., Arno, M.C., Ruipérez, F., Hedrick, J.L., Dove, A.P.,
666 Sardon, H., 2020. Synthesis of Functionalized Cyclic Carbonates through Commodity Polymer
667 Upcycling. *ACS Macro Lett.* 9, 443-447. <https://doi.org/10.1021/acsmacrolett.0c00164>.
668
- 669 Jiang, S., Cheng, H., Shi, R., Wu, P., Lin, W, Zhang, C., Arai, M., Zhao, F., 2019. Direct Synthesis
670 of Polyurea Thermoplastics from CO₂ and Diamines. *ACS Applied Materials & Interfaces* 11 (50),
671 47413-47421. <https://doi.org/10.1021/acсами.9b17677>.
672
- 673 Jones, G.O., Yuen, A., Wojtecki, R.J., Hedrick, J.L., Garcia, J.M., 2016. Computational and
674 experimental investigations of one-step conversion of poly(carbonate)s into value-added poly(aryl
675 ether sulfone)s. *Natl. Acad. Sci. U. S. A.* 28, 7722-7726. <https://doi.org/10.1073/pnas.1600924113>.
676
- 677 Kébir, N., Benoit, M., Legrand, C., Burel, F., 2017. Non-isocyanate thermoplastic polyureas
678 (NIPUreas) through a methyl carbamate metathesis polymerization. *Eur. Polym J.* 96, 87-96.
679 <https://doi.org/10.1016/j.eurpolymj.2017.08.046>.

- 680 Kim, J.G., 2020. Chemical recycling of poly(bisphenol A carbonate). *Polym. Chem.*
681 <https://doi.org/10.1039/C9PY01927H>.
682
- 683 La Mantia, F. (Ed.), 2002. *Handbook of Plastic Recycling*. Rapra Technology, Shrewsbury, U.K.
684
- 685 Li, S., Han, H., Zhu, X., Jiang, X., Kong, X.Z., 2015. Preparation and Formation Mechanism of
686 Porous Polyurea by Reaction of Toluene Diisocyanate with Water and Its Application as Adsorbent
687 for Anionic Dye Removal. *Chinese J. Polymer Sci.* 33, 1196-1210. [https://doi.org/10.1007/s10118-](https://doi.org/10.1007/s10118-015-1670-7)
688 [015-1670-7](https://doi.org/10.1007/s10118-015-1670-7).
689
- 690 Liu, M., Guo, J., Gu, Y., Gao, J., Liu, F., 2018. Degradation of waste polycarbonate via hydrolytic
691 strategy to recover monomer (bisphenol A) catalyzed by DBU-based ionic liquids under metal- and
692 solvent-free conditions. *Polym. Degrad. Stab.* 157, 9-14.
693 <https://doi.org/10.1016/j.polymdegradstab.2018.09.018>.
694
- 695 Liu, F., Guo, J., Zhao, P., Jia, M., Liu, M., Gao, J., 2019. Novel succinimide-based ionic liquids as
696 efficient and sustainable media for methanolysis of polycarbonate to recover bisphenol A (BPA)
697 under mild conditions. *Polym. Degrad. Stab.* 108996.
698 <https://doi.org/10.1016/j.polymdegradstab.2019.108996>.
699
- 700 Lortie, F., Boileau, S., Bouteiller, L., 2003. N,N-Disubstituted Ureas: Influence of Substituents on
701 the Formation of Supramolecular Polymers. *Chem. Eur. J.* 9, 3008 – 3014 and refs therein.
702 <https://doi.org/10.1002/chem.200304801>.
703

704 Ma, S., van Heeswijk, E.P.A., Noordover, B.A.J., Sablong, R.J., van Benthem, R.A.T.M., Koning,
705 C.E., 2018. Isocyanate-Free Approach to Water-Borne Polyurea Dispersions and Coatings.
706 ChemSusChem. 11, 149-158. <https://doi.org/10.1002/cssc.201701930>.

707

708 Mattia, J., Painter, P., 2007. A comparison of hydrogen bonding and order in a polyurethane and
709 poly(urethane-urea) and their blends with poly(ethylene glycol). Macromolecules. 40, 1546-1554.
710 <https://doi.org/10.1021/ma0626362>.

711

712 Mido, Y., 1972. Infrared spectra and configurations of dialkylureas. Spectrochimica Acta. 28A,
713 1503-1518. [https://doi.org/10.1016/0584-8539\(72\)80120-X](https://doi.org/10.1016/0584-8539(72)80120-X).

714

715 Mido, Y., 1973. An infrared study of various dialkylureas in solution. Spectrochimica Acta. 29A,
716 431-438. [https://doi.org/10.1016/0584-8539\(73\)80025-X](https://doi.org/10.1016/0584-8539(73)80025-X).

717

718 Monsigny, L., Berthet, J.-C., Cantat, T., 2018. Depolymerization of Waste Plastics to Monomers
719 and Chemicals Using a Hydrosilylation Strategy Facilitated by Brookhart's Iridium(III) Catalyst.
720 ACS Sustainable Chem. Eng. 6, 10481-10488. <https://doi.org/10.1021/acssuschemeng.8b01842>.

721

722 Pan, W.C., Liao, K., Lin, C.-H., Dai, S.A., 2015. Solvent-free processes to polyurea elastomers
723 from diamines and diphenyl carbonate. J. Polym. Res. 22, 114. [https://doi.org/10.1007/s10965-](https://doi.org/10.1007/s10965-015-0747-x)
724 [015-0747-x](https://doi.org/10.1007/s10965-015-0747-x).

725

726 Perrin, D.D., Armarego, W.L.F., Perrin, D.R., 1986. Purification of Laboratory Chemicals.
727 Pergamon, Oxford.

728

- 729 Pires, R.F., Bonifacio, V.D.B., 2000. Polyureas, in: Kirk-Othmer Encyclopedia of Chemical
730 Technology. John Wiley & Sons, Inc. <https://doi.org/10.1002/0471238961.koe00032>.
731
- 732 Quaranta, E., 2017. Rare Earth metal triflates $M(O_3SCF_3)_3$ ($M = Sc, Yb, La$) as Lewis acid catalysts
733 of depolymerization of poly-(bisphenol A carbonate) via hydrolytic cleavage of carbonate moiety:
734 Catalytic activity of $La(O_3SCF_3)_3$. *Appl. Catal. B Environ.* 206, 233-241.
735 <https://doi.org/10.1016/j.apcatb.2017.01.007>.
736
- 737 Quaranta, E., Sgherza, D., Tartaro, G., 2017. Depolymerization of poly(bisphenol A carbonate)
738 under mild conditions by solvent free alcoholysis catalyzed by 1,8-diazabicyclo[5.4.0]undec-7-ene
739 as a recyclable organocatalyst: a route to chemical recycling of waste polycarbonate. *Green Chem.*
740 19, 11-16. <https://doi.org/10.1039/C7GC02063E>.
741
- 742 Quaranta, E., Castiglione Minischetti, C., Tartaro, G., 2018. Chemical recycling of poly(bisphenol
743 A carbonate) by glycolysis under 1,8-diazabicyclo[5.4.0]undec-7-ene catalysis. *ACS Omega* 3,
744 7261-7268. <https://doi.org/10.1021/acsomega.8b01123>.
745
- 746 Ragaert, K., Delva, L., Van Geem, K., 2017. Mechanical and chemical recycling of solid plastic
747 waste. *Waste Manage.* 69, 24–58. <https://doi.org/10.1016/j.wasman.2017.07.044>.
748
- 749 Rahimi, A.R., García, J.M., 2017. Chemical recycling of waste plastics for new materials
750 production. *Nat. Rev. Chem.* 1, 41570-41580. <https://doi.org/10.1038/s41570-017-0046>.
751
- 752 Rokicki, G., 1988. Direct method of synthesis of polyureas by N-acylphosphoramidites. *Makromol.*
753 *Chem.* 189, 2513-2520. <https://doi.org/10.1002/macp.1988.021891101>.

- 754 Shang, J., Liu, S., Ma, X., Lua, L., Deng, Y., 2012. A new route of CO₂ catalytic activation:
755 syntheses of N-substituted carbamates from dialkyl carbonates and polyureas. *Green Chem.* 14,
756 2899-2906. <https://doi.org/10.1039/C2GC36043H>.
757
- 758 Shao, S.W., Chen, H.C., Chan, J.R., Juang, T.Y., Abu-Omar, M.M., Lin, C.H., 2020. Full atom-
759 efficiency transformation of wasted polycarbonates into epoxy thermosets and the catalyst-free
760 degradation of the thermosets for environmental sustainability. *Green Chem.* 22, 4683-4696.
761 <https://doi.org/10.1039/d0gc01318h>.
762
- 763 Shawali, A.S., Harhash, A., Sidky, M.M., Hassaneen, H.M., Elkaabi, S.S., 1986. Kinetics and
764 Mechanism of Aminolysis of Carbamates. *J. Org. Chem.* 51, 3498-3501.
765 <https://doi.org/10.1021/jo00368a020>.
766
- 767 Singh, S., Leib, Y., Schober, A., 2015. Direct extraction of carbonyl from waste polycarbonate
768 with amines under environmentally friendly conditions: scope of waste polycarbonate as a
769 carbonylating agent in organic synthesis. *RSC Adv.* 5, 3454-3460.
770 <https://doi.org/10.1039/C4RA14319A>.
771
- 772 Socrates, G., 2001. *Infrared and Raman Characteristic Group Frequencies*, third ed. John Wiley &
773 Sons, LTD, Chichester, England, pp. 151-154.
774
- 775 Taguchi, M., Ishikawa, Y., Kataoka, S., Naka, T., Funazukuri, T., 2016. CeO₂ nanocatalysts for the
776 chemical recycling of polycarbonate. *Catal. Commun.* 84, 93-97.
777 <https://doi.org/10.1016/j.catcom.2016.06.009>.
778

779 Tang, H., Hu, T., Li, G., Wang, A., Xu, G., Yu, C., Wang, X., Zhang, T., Li, N., 2019. Synthesis of
780 jet fuel range high-density polycycloalkanes with polycarbonate wast. *Green Chem.* 21, 3789-3795.
781 [https://doi.org/ 10.1039/c9gc01627a](https://doi.org/10.1039/c9gc01627a).

782

783 Tucker, D.K., Hayes Bouknight, S., Brar, S.S., Kissling G.E., Fenton, S.E., 2018. Evaluation of
784 Prenatal Exposure to Bisphenol Analogues on Development and Long-Term Health of the
785 Mammary Gland in Female Mice. *Environ. Health Perspect.* 126, 087003.
786 <https://doi.org/10.1289/EHP3189>.

787

788 Um, I.-H., Song, J.-H., Bae, A.-R., Dust, J.M., 2018. Unexpected medium effect on the mechanism
789 for aminolysis of aryl phenyl carbonates in acetonitrile and H₂O: transition-state structure in the
790 catalytic pathway. *Can. J. Chem.* 66, 1011-1020. <https://doi.org/10.1139/cjc-2018-0204>.

791

792 Wang, P., Ma, X., Li, Q., Yang, B., Shang, J., Deng, Y., 2016. Green synthesis of polyureas from
793 CO₂ and diamines with a functional ionic liquid as the catalyst. *RSC Adv.* 6, 54013-54019.
794 <https://doi.org/10.1039/C6RA07452A>.

795

796 Wang, J., Jiang, J., Wang, X., Wang, R., Wang, K., Pang, S., Zhong, Z., Sun, Y., Ruan, R.,
797 Ragauskas, A.J., 2020. Converting polycarbonate and polystyrene plastic wastes into aromatic
798 hydrocarbons via catalytic fast co-pyrolysis. *J. Hazard. Mater.* 386, 121970.
799 <https://doi.org/10.1016/j.jhazmat.2019.121970>.

800

801 Westhues, S., Idel, J., Klankermayer, J., 2018. Molecular catalyst systems as key enablers for
802 tailored polyesters and polycarbonate recycling concepts. *Sci. Adv.* 4(8), eaat9669.
803 <https://doi.org/10.1126/sciadv.aat9669>.

804

805 Wu, C., Wang, J., Chang, P., Cheng, H., Yu, Y., Wu, Z., Dong, D., Zhao, F., 2012. Polyureas from
806 diamines and carbon dioxide: synthesis, structures and properties. *Phys. Chem. Chem. Phys.* 14,
807 464–468. <https://doi.org/10.1039/C1CP23332G>.

808

809 Wu, C.-H., Chen, L.-Y., Jeng, R.-J., Dai, S.A., 2018. 100% Atom-economy efficiency of recycling
810 polycarbonate into versatile intermediates. *ACS Sustainable Chem. Eng.* 6, 8964-8975.
811 <https://doi.org/10.1021/acssuschemeng.8b01326>.

812

813 Yilgor, E., Burgaz, E., Yurtsever, E., Yilgor, I., 2000. Comparison of hydrogen bonding in
814 polydimethylsiloxane and polyether based urethane and urea copolymers. *Polymer.* 41, 849–857.
815 [https://doi.org/10.1016/S0032-3861\(99\)00245-1](https://doi.org/10.1016/S0032-3861(99)00245-1).

816

817 Ying, Z., Zhao, L., Zhang, C., Yu, Y., Liu, T., Cheng, H., Zhao, F., 2015. Utilization of carbon
818 dioxide to build a basic block for polymeric materials: an isocyanate-free route to synthesize a
819 soluble oligourea. *RSC Adv.* 5, 42095–42100. <https://doi.org/10.1039/C5RA02819A>.

820